Indian Journal of Pure & Applied Physics
Vol. 57, January 2019, pp. 7-13

One step synthesis of Cu_2ZnSnS_4 nanoflakes by microwave irradiation technique and effect of Cu concentration

S P Kandare, A B Thorat, S D Dhole & S S Dahiwale*

Department of Physics, Savitribai Phule Pune University, Pune 411 007, India

Received 26 June 2017; accepted 23 August 2018

The influence of cyclic microwave irradiation and effect of Cu concentration has been investigated for synthesis of pure phase Cu_2ZnSnS_4 powder. It has been observed that Cu concentration plays a vital role to get pure phase Cu_2ZnSnS_4. The optical properties, phase purity, crystallographic structure and morphology have been investigated by spectroscopic and microscopic techniques. The results reveal that single phase kesterite Cu_2ZnSnS_4 with no other secondary phase can be obtained by precisely controlling the cyclic microwave irradiation time and the precursor concentrations. The optical band gap of prepared Cu_2ZnSnS_4 powder, estimated from UV-Visible spectroscopy has been found to be ~ 1.45 eV which is superlative for photovoltaic application. Systematic Raman study confirms the formation of Cu_2ZnSnS_4 phase and suppression of CuS peak with proper control in copper concentration. TEM image shows nanoflakes kind of morphology having thickness of flakes between 25 nm to 45 nm. Further the crystal inter-planer spacing is found to be 0.32 nm, which is consistent with the XRD data and ascribed to (112) plane.

Keywords: CZTS, Nanoflakes, UV-Visible, XRD, Raman spectroscopy, TEM, FESEM

1 Introduction

Cu_2ZnSnS_4 is the I_2 -II- IV- VI_4 quaternary compound which has emerged as a promising compound for photo absorbing material in PV technology, due to its high absorption coefficient of 10^4 cm^{-1}. CZTS is *p*-type semiconductor with a band gap ranging from 1.0 eV to 1.5 eV, suitable for maximum solar radiation absorption. CZTS consists of earth abundant, non-toxic and inexpensive materials and therefore it can be made more affordable compared to other thin film solar cells. The maximum solar cell efficiency in lab scale achieved using CZTS[1] is around 12% and that of CZTSSe material[2] is 12.6%. Both vacuum and non vacuum techniques can be exploited for synthesis of CZTS material. Vacuum technique requires expensive instrumentation, whereas non vacuum techniques are comparatively much more inexpensive. However, one can easily maintain quality and stability of films in vacuum technique, whereas many efforts are required in the case of non vacuum technique. Today's demand is to make the solar power generation to be affordable and that's why non vacuum process is more feasible. There are various non-vacuum techniques such as electro-deposition[3-8], screen printing[9,10], spray pyrolysis technique[11-15], sol-gel[11-19] etc. which are applied by various research groups to prepare the CZTS thin films in order to reduce the cost and simplify the fabrication process of complete thin film solar cell.

We used microwave assisted synthesis method which is one of the techniques in nano synthesis of material. The microwave technique is unique as compared to other non vacuum technique. Microwave synthesis enhances materials quality and controls size due to its characteristic properties like highly accelerated rate of reaction, uniform heating, reaction homogeneity which empower homogeneous nucleation and growth, smaller particle size and reproducibility[20-24]. Microwave assisted synthesis are faster, cleaner and more economical than the conventional method.

In the present work, pure phase Cu_2ZnSnS_4 was synthesized using microwave synthesis method. The domestic microwave oven having power output 1200-watt was utilized for synthesis of CZTS. Five samples investigated by increasing cyclic microwave irradiation from 3 to 15 cycles (where one cycle represents on time 60 sec and off time 60 sec) keeping the proportion of precursors copper, zinc, tin and sulfur at around 2:1:1:4. Further, we investigated the effect of copper concentration on the optimized microwave irradiated sample.

*Corresponding author (E-mail: ssd@physics.unipune.ac.in)

2 Experimental Details

The elemental precursors of copper, zinc, tin and sulfur was added in stoichiometric ratio of 2:1:1:4 in 50 mL ethylene glycol. This solution was then stirred for about 2 h. During the stirring process, color of solution changed from yellow to colorless. The colorless mixture solution was then subjected to microwave irradiation at varying ON/OFF cycle. After microwave irradiation the mixture solution was allowed to cool down to room temperature naturally. Thereafter, solution was washed using ethanol and distilled water for at least ten times to get the precipitate. Finally the precipitate was baked which turned into black powder.

In order to study the effect of microwave irradiation and copper concentration, two sets of experiments were carried out. In the first set, cyclic microwave irradiation was carried out for 3 cycles, 6 cycles, 9 cycles, 12 cycles and 15 cycles. Here one complete cycle refers as 60 s ON /60 s OFF time. Thus we prepared five samples, S1, S2, S3, S4 and S5 representing to microwave irradiation of 3, 6, 9, 12 and 15 cycles, respectively, keeping the precursors concentration of Cu, Zn, Sn and S in a ratio of 2:1:1:4.

In the second set, the copper concentration was reduced systematically as 3 mM (the sample named as S6), 2.8 mM (S7), 2.6 mM (S8) and 2.4 mM (S9), keeping the precursors concentration of Zn, Sn and S constant. All the samples thus obtained were used for further characterizations.

Optical absorption measurement was carried out in the wavelength range of 300 nm to 1000 nm using UV Visible spectrometer JASCO V 670. The crystal structure and crystallite size of the sample was determined from an X-Ray diffractometer (1.54 Å) with Cu Kα ray using D8 Advance BRUKER AXS. Raman spectroscopic measurements were carried out at the excitation wavelength of 532 nm using RENISHAW in Via UPE II. Surface morphology and crystal inter-planer distance of the sample was examined by FESEM NOVA NANOSEM 450 FEI and TEM Tecnai G2 U-Twin 200kV Lab6 FEI, respectively.

3 Results and Discussion

3.1 Effect of cyclic irradiation

Figure 1 shows UV absorbance spectra of microwave irradiated samples S1, S2, S3, S4, and S5. Figure 2 shows the Tauc's plots of respective S1, S2, S3, S4 and S5 sample. Results show that the optical band gap decreases from 1.95 eV to 1.45 eV with increase in microwave cyclic irradiation from 3 cycles to 15 cycles, i.e., for S1 to S5 samples. The band-gap for S4 and S5 are well in agreement with the previously reported values[25,26] of CZTS material. It has been confirmed by various researchers that during the synthesis of CZTS from the precursors, nucleation initially begins with secondary phases such as ZnS, SnS_2, Cu_2S, CuS, Cu_2SnS_3 etc. which then take over by CZTS phase[27-29]. Literature[30] reveals that the band-gap of CuS crystals can vary between 1.9 eV to 1.6 eV. For other secondary phases the band-gap for ZnS[31,32] varies between 4.2 eV to 3.6 eV, for SnS_2[33] varies between 2.06 eV to 1.76 eV, for Cu_2S[30,34] varies from 1.9 eV to 1.3 eV and for Cu2ZnS varies

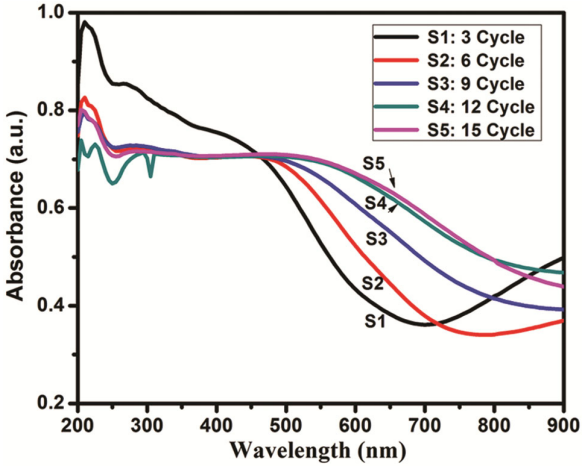

Fig. 1 – UV spectra of CZTS powder synthesized by microwave irradiation at different cyclic irradiation.

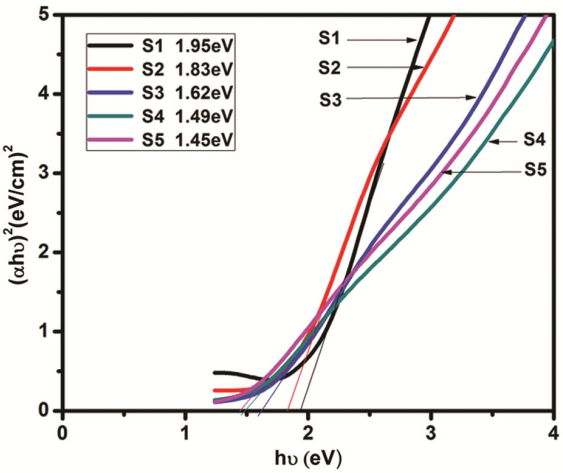

Fig. 2 – Tauc's plot of CZTS powder synthesized by microwave irradiation at different cyclic irradiation.

from 1.6 eV to 1.19 eV. We believe that in our case, initially for lower microwave cyclic irradiation the nucleation of CuS or Cu2S particles are more dominant and as we increase the microwave irradiation cycle the CZTS phase starts over it. Usually the particle size is correlated with the band gap as the particle size reduces the band-gap increases. However with increase in microwave irradiation time the band-gap is decreasing so we can neglect the possibility of reduction of CuS or CuS2 particle size. Thus UV-Visible spectra tell the possibilities of various phases. We have systematically eliminated all other possible phases except CuS and CZTS, which has been explained in the subsequent analysis. From UV-visible spectra we assume that shift in the band gap can be due to more and more growth of CZTS crystals as compared to other impurity phases as we go on increase in the cyclic microwave irradiation. These results suggest that the microwave cyclic irradiation is playing crucial role in controlling the phases and band gap of the synthesizing material.

Figure 3 shows the XRD graphs of the S1, S2, S3, S4 and S5 samples. For S1, S2 and S5 samples the diffraction peaks appeared to be at 27.7°, 31.8°, 52.5°, 57.28°, 59.1° which are attributed to the binary CuS phases (JCPDS card No. 85-0620). Whereas, for S3 and S4 samples XRD curve exhibits four broad peaks at 28.6°, 32.8°, 47.5° and 56.3° assigned to (112), (200), (220), (312) planes of kesterite type CZTS which are well matched with the JCPDS card No. 26-0575. However, the above peak positions of sample S3 and S4 also represents ZnS (JCPDS card No. 80-0020) and Cu_2SnS_3 (JCPDS card No. 27-0198). For S1, S2 and S5 samples we can clearly see from figure mixed phases of CZTS and CuS are present. Therefore, pure phase of CZTS cannot be confirmed only by XRD and UV-visible measurements. In order to confirm whether pure phase CZTS was formed, Raman spectroscopy was carried out on these samples.

Figure 4 shows the Raman spectra of S1, S2, S3, S4 and S5 samples. It can be observed from Figure 4 that there is a small peak at around 470 cm^{-1} along with the peak at 331 cm^{-1} for all the five samples. The 331 cm^{-1} peak is a signature peak of CZTS[35], however the peak at 470 cm^{-1}represents CuS[36]. Further, it can be clearly seen that for sample S1, CuS is more intense and CZTS signature peak is very weak. However for samples S2, S3, S4 and S5, the CZTS peak intensity has increased substantially along with non-negligible peak of CuS. To get more quantitative information, we estimated the relative percentage change in CuS peak to that of CZTS peak by evaluating their area under the curves. It has been observed that with increase in the microwave cyclic irradiation time the percentage of CuS phase has gone down to 1% for S4 sample compared to 61% for S1 sample. The Raman results are in agreement with the UV and XRD results. These results clearly imply that cyclic microwave irradiation plays a vital role in formation of CZTS phase, however one has to properly control the microwave irradiation time to obtain the CZTS phase. From these results, we can

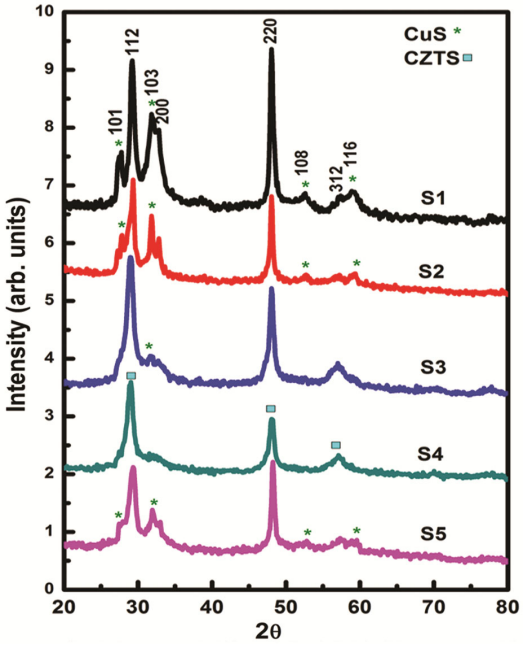

Fig. 3 – XRD spectra of CZTS powder synthesized by microwave irradiation at different cyclic irradiation.

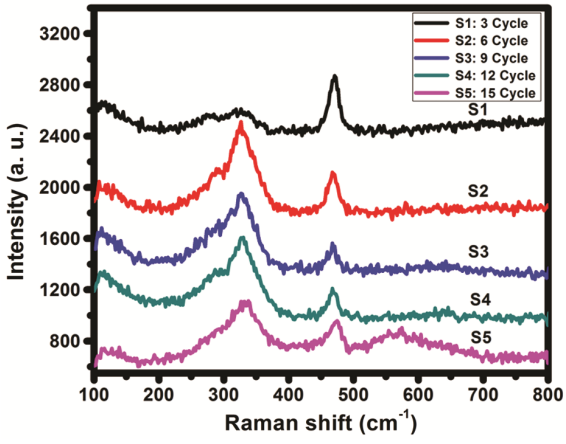

Fig. 4 – Raman spectra of CZTS powder synthesized at different time cycles of microwave irradiation.

confirm that with cyclic microwave irradiation, initially there is a formation of mixed phases of CZTS and CuS. However, when we increase the cyclic irradiation time, more intense peak of CZTS appear revealing the formation of CZTS phase more compared to secondary CuS.

Correlating Raman data with XRD and UV-visible data, we observed that up to 12 cycles there is systematic appearance of CZTS phases however after that, the sample shows the unwanted secondary phases in combination with CZTS and CuS. So to obtain pure phase of CZTS, we kept 12 cycles as our optimized condition for microwave irradiation and systematically decreased the Cu concentration from 3 mM to 2.4 mM.

3.2 Effect of Cu concentration

Figure 5 shows UV absorption spectra of CZTS powder synthesized by 12 cycles of microwave irradiation at decreasing copper concentrations of 3 mM (S6), 2.8 mM (S7), 2.6 mM (S8) and 2.4 mM (S9). Figure 6 shows the respective Tauc's plot of CZTS powder at different copper concentrations. The optical band gap increases from 1.33eV to 1.45eV with decrease in copper concentration, i.e., for S6 to S8 samples. The band gap for S9 is well in agreement with the previously reported values[25,26] of CZTS material.

Figure 7 shows XRD graphs of the samples S6, S7, S8 and S9, which exhibits four broad XRD peaks assigned to (112), (200), (220), (312) planes of kesterite type CZTS which are in accordance with above XRD results.

Figure 8 shows Raman spectra of the CZTS samples prepared at different copper concentrations. As we have already discuss, the 331 cm^{-1} peak is a signature peak of CZTS, however the peak at around 470 cm^{-1} is for CuS. It can be clearly observed from figure that with lowering the copper concentration the peak intensity of CuS was decreasing gradually, and vanished at a copper concentration of 2.4 mM. The relative percentage change of CuS phase in to the

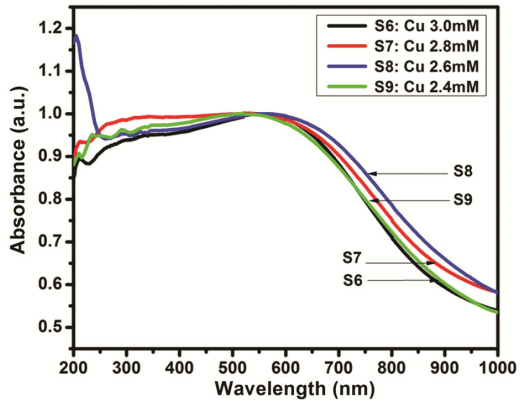

Fig. 5 – UV spectra of CZTS powder synthesized by microwave irradiation at different copper concentration.

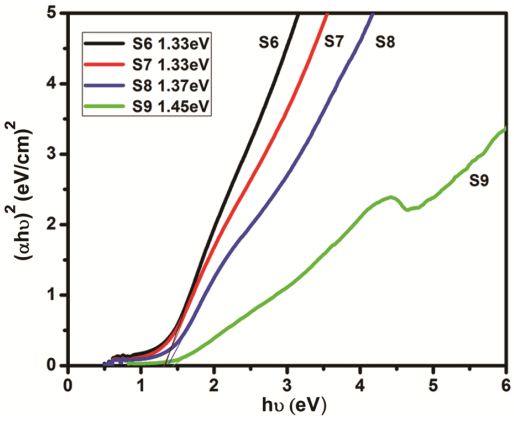

Fig. 6 – Tauc's plot of CZTS powder synthesized by microwave irradiation at different copper concentration.

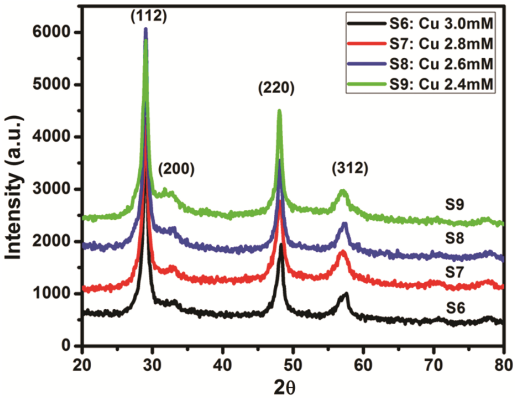

Fig. 7 – XRD spectra of CZTS powder synthesized by microwave irradiation at different copper concentration.

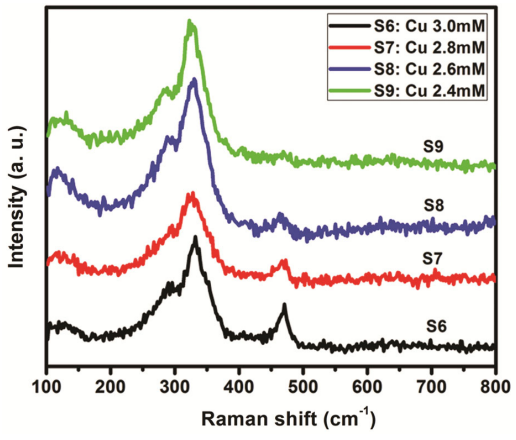

Fig. 8 – Raman spectra of CZTS powder synthesized by microwave irradiation at different copper concentration.

CZTS was again calculated. It was observed that reduction of Cu concentration the percentage change of CuS phase in CZTS was decreasing sharply and for S9 sample CuS peak completely vanished. Thus we were successful in elimination of the secondary CuS phase and getting the pure CZTS phase. This confirmation was obtained only due to Raman analysis and wouldn't have been possible only on the basis of XRD and optical absorption measurements

Figure 9 shows Raman spectra of the optimized pure phase CZTS sample. At ambient temperature CZTS has following formula for normal lattice vibrations at zone centre Γ in the Brillouin zone.

$\Gamma_{optic} = 3A(R) + 6B(R, IR) + 3E_1(R, IR) + 3E_2(R, IR)$.

Due to selection rule for Raman and IR at zone center q≈ 0 only optics modes are investigate in Raman spectroscopy. Out of 21 Raman active modes, we have observed only 4 modes. The reason for observing less number of modes than expected could be due to weak modes or accidently degeneracy. The peaks at 331 cm^{-1}, 288 cm^{-1}, 269 cm^{-1}, 350 cm^{-1} are due to A1, A2, A3 and B modes[37]. Many reports suggest for CZTS single crystal[38] the signature peak stands at 338cm^{-1}. As compared to our data this peak shifts toward (331 cm^{-1}) lower frequency, this decrease in Raman shift is due to decrease in A1 mode as asymmetric broadening and shift in Raman line depends on particle size[35].

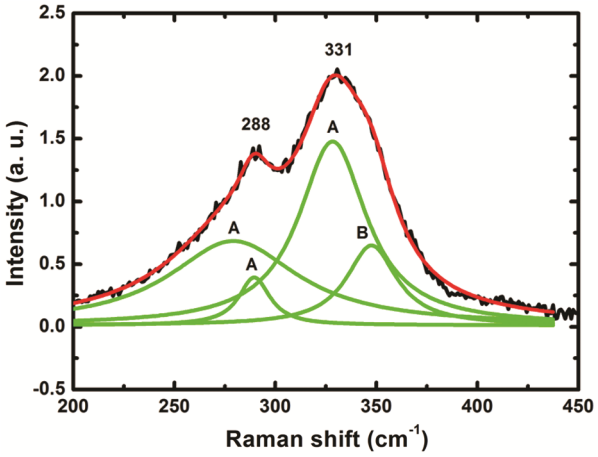

Fig. 9 – Raman spectra of CZTS powder at ambient temperature.

Thus from the above result we confirm that the pure CZTS phase sample can be obtain for 12 cycle of microwave irradiation and keeping the concentration of Cu, Zn, Sn, and sulphur at 2.5 mM, 2.4 mM, 2.0 mM and 9 mM, respectively. From Fig. 7, the average crystallite size of the best sample was estimated to be around 19 nm, using the standard Debye Scherrer formula[39].

Furthermore we analyzed our best sample with TEM and FESEM. For TEM investigation, sample was dispersing in ethanol, drop coated on copper-carbon TEM grid and dried at room temperature for 24 h before taking the measurements. Figure 10 (a) and (b) shows the TEM images of CZTS sample. From Fig. 10 (a), we observed a nanoflakes kind of morphology and Fig. 10 (b) reveals the crystal inter-planer spacing of 0.32 nm, which is in agreement with the XRD data ascribed to the (112) plane. **Fig**ure 11 (a) and (b) shows FESEM images of synthesized CZTS powder. From the figure it can be observed that these nanoflakes are having thickness of flakes between 25 nm to 45 nm. The growth of flake like structures can be due to the CuS nucleation at the

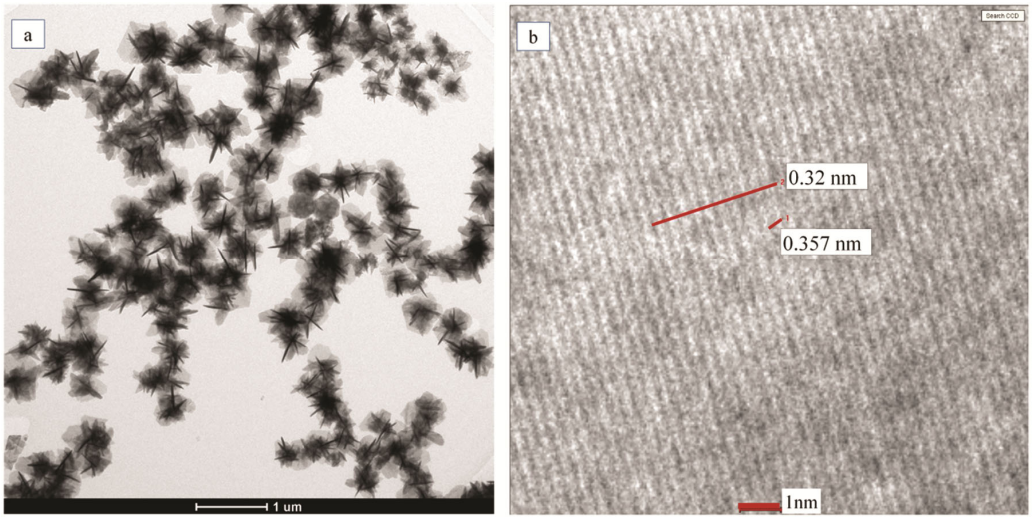

Fig. 10 – TEM images of CZTS powder synthesized by microwave irradiation method (a) TEM image and (b) inter-planner spacing image.

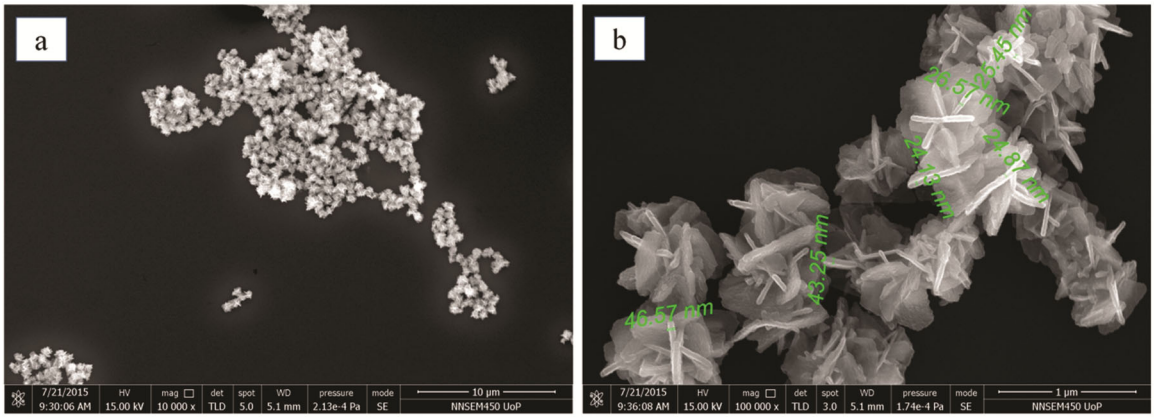

Fig. 11 – FESEM images of CZTS powder synthesized by microwave irradiation method at optimised condition.

initial stages of microwave irradiation, the CuS grows in preferential direction and these nuclei prefers to grow in flake like crystal structures[40,41]. As we increase the microwave irradiation cycle, the CZTS crystal grows CuS on while reacting with CuS. Similar growth mechanisms have also been observed by few other researchers[42-44]. This kind of morphology can be useful for getting the high efficiency of solar cells, as such morphology will provide high surface to volume ratio. It was also been seen in literature that such 2D nanosheets or nanoflakes improves many physical properties which can help in improving the device performances[45-47].

4 Conclusions

In conclusion, CZTS powder was synthesized using one step microwave irradiation method. The physical properties such as structural, morphological and optical absorption was done using XRD, Raman, TEM, FESEM and UV Visible spectroscopy. Experimentally it is quite difficult to obtained pure CZTS phase, however pure phase CZTS was obtained from mixed phases of CuS and CZTS by properly controlling the cyclic microwave irradiation and Cu concentration. TEM and FESEM analysis confirms the nanoflake like morphology. Thus using microwave irradiation pure phase CZTS crystal can be prepared quickly and efficiently at very low cost. The synthesized powder shows all the promising properties of absorbing layer, thus it can be used for thin-film solar cells.

Acknowledgement

The authors appriciate PU-BARC MoU, UGC start-up grant for some financial support to carry out this work. Authors are also thankful for the financial support from UGC-UPE phase-II project to further continue this work. Authors also acknowledge Dr Mala Rao and Dr Rekha Rao from Solid State Physics Division, Bhabha Atomic Research Centre for the discussions.

References

1 Xiangbo Song H Z, Ji X, Li M, Lin W & Luo X, *Int J Photoenergy*, 2014 (2014) 11.
2 Wang W, Winkler M T, Gunawan O, Gokmen T, Todorov T K, Zhu Y & Mitzi D B, *Adv Energy Mater*, 4 (2014) 1.
3 Rao M C, Sk Shahenoor B, *Res Phys*, 9 (2018) 996.
4 Araki H, Kubo Y, Jimbo K, Maw W S, Katagiri H, Yamazaki M, Oishi K & Takeuchi A, *Phys Status Solidi Curr Top Solid State Phys*, 6 (2009) 1266.
5 Ennaoui A, Lux-Steiner M, Weber A, Abou-Ras D, Kötschau I, Schock H W, Schurr R, Hölzing A, Jost S, Hock R, Vob T, Schulze J & Kirbs A, *Thin Solid Films*, 517 (2009) 2511.
6 Scragg J J, Berg D M & Dale P J, *J Electroanal Chem*, 646 (2010) 52.
7 Schurr R, Hölzing A, Jost S, Hock R, Vob T, Schulze J, Kirbs A, Ennaoui A, Lux-Steiner M, Weber A, Kötschau I & Schock H W, *Thin Solid Films*, 517 (2009) 2465.
8 Zhou Z, Wang Y, Xu D & Zhang Y, *Sol Energy Mater Sol Cells*, 94 (2010) 2042.
9 Kumar V, Padhy S, Basak A & Singh U P, *Vacuum*, 155 (2018) 336.
10 Nakayama N & Ito K, *Appl Surf Sci*, 92 (1996) 171.
11 Babichuk I S, Golovynskyi S, Brus V V, Babichuk I V, Datsenko O, Li J, Xu G, Golovynska I, Hreshchuk O M, Orletskyi I G, Qu J, Yukhymchuk V O, Maryanchuk P D, *Mater Lett*, 216 (2018) 173.
12 Zhong M, Liu S, Li H & Li C, *Chalcogenide Lett*, 15 (2018) 133.
13 Kamoun N, Bouzouita H & Rezig B, *Thin Solid Films*, 515 (2007) 5949.
14 Kumar Y B K K, Bhaskar P U, Babu G S & Raja V S, *Phys Status Solidi Appl Mater Sci*, 207 (2010) 149.
15 Yeh M Y, Lee C C & Wuu D S, *J Sol gel Sci Technol*, 52 (2009) 65.
16 Dong L, Cheng S, Lai Y, Zhang H & Jia H, *Thin Solid Films*, 626 (2017) 168.

17 Moritake N, Fukui Y, Oonuki M, Tanaka K & Uchiki H, *Phys Status Solidi Curr Top Solid State Phys*, 6 (2009) 1233.
18 Tanaka K, Fukui Y, Moritake N & Uchiki H, *Sol Energy Mater Sol Cells*, 95 (2011) 838.
19 Maeda K, Tanaka K, Fukui Y & Uchiki H, *Sol Energy Mater Sol Cells*, 95 (2011) 2855.
20 Patro B, Vijaylakshmi S & Sharma P, *J Mater Sci Mater Electron*, 29 (2018) 3370.
21 Flynn B, Wang W, Chang C H & Herman G S, *Phys Status Solidi Appl Mater Sci*, 209 (2012) 2186.
22 Saravana Kumar R, Ryu B D, Chandramohan S, Seol J K, Lee S K & Hong C H, *Mater Lett*, 86 (2012) 174.
23 Zhou Z, Zhang P, Lin Y, Ashalley E, Ji H, Wu J, Li H & Wang Z, *Nanoscale Res Lett*, 9 (2014) 2.
24 Martini T, Chubilleau C, Poncelet O, Ricaud A, Blayo A, Martin C & Tarasov K, *Sol Energy Mater Sol Cells*, 144 (2016) 657.
25 Calvet I, Barrachina E, Mart R, Fraga D, Lyubenova T S & Carda J B, *Bol La Soc Esp Ceram Y Vidr*, 54 (2015) 175.
26 Isah K U, Yabagi J A, Ahmadu U, Isah M, Gaetan M, Kana Z & Oberafo A A, *IOSR J Appl Phys*, 2 (2013) 14.
27 Scragg J J, Ericson T, Kubart T, Edoff M & Platzer-Bjorkman C, *Chem Mater*, 23 (2011) 4625.
28 Aditha S K, Kurdekar A D, Avinash Chunduri L A, Patnaik S & V Kamisetti, *Methods X*, 3 (2016) 35.
29 Tiing Tiong V, Bell J & Wang H, *Beilstein J Nanotechnol*, 5 (2014) 438.
30 Tanveer M, Cao C, Aslam I, Ali Z, Idrees F, Tahir M, Khan W S, Butt F K & Mahmood A, *RSC Adv*, 4 (2014) 63447.
31 Maity R & Chattopadhyay K K, *Nanotechnology*, 15 (2004) 812.
32 Kanti Kole A & Kumbhakar P, *Res Phys*, 2 (2012) 150.
33 Lin C, Zhu M Zhang, T, Liu Y, Lv Y, Li X & Liu M, *RSC Adv*, 7 (2017) 12255.
34 Pop A E, *Chalcogenide Lett*, 8 (2011) 363.
35 Zhao Y, Tao W, Chen X, Liu J & Wei A, *J Mater Sci Mater Electron*, 26 (2015) 5645.
36 Isac L A, Duta A, Kriza A, Enesca I A & Nanu M, *J Phys Conf Ser*, 61 (2007) 477.
37 Pandey S D, Samanta K, Singh J & Sharma N D, *Int J Adv Electron Commun Eng*, 3 (2014) 317.
38 Guc M, Levcenko S, Bodnar I V, Izquierdo-roca V, Fontane X, Volkova L V, Arushanov E & Pérez Rodríguez A, *Sci Rep*, 5 (2016) 19414.
39 Alexander L & Klug H P, *J Appl Phys*, 21 (1950) 137.
40 Banerjee N, *Mater Chem Phys*, 137 (2012) 466.
41 U Shamriaz, *J Solid State Chem*, 238 (2016) 25.
42 Zhai X, *Crys Eng Commun*, 16 (2014) 6244.
43 Zhang X, *Cryst Eng Commun*, 20 (2018) 2351.
44 Saranya M, *J Nano Res*, 18 (2012) 43.
45 Donahoe F J, *J Franklin Inst*, 271 (2014) 230.
46 Zhou Y L, Zhou W H, Li M, Du Y F & Wu S X, *J Phys Chem C*, 115 (2011) 19632.
47 Shi Y, Zhu C, Wang L, Zhao C, Li W, Fung K K, Ma T, Hagfeldt A & Wang N, *Chem Mater*, 25 (2013) 1000.